Analytical Methods

ROYAL SOCIETY OF CHEMISTRY

PAPER

View Article Online
View Journal | View Issue

Cite this: *Anal. Methods*, 2021, **13**, 789

Facile synthesis of biomass waste-derived fluorescent N, S, P co-doped carbon dots for detection of Fe^{3+} ions in solutions and living cells†

Weixia Wang, Jie Chen, Dake Wang, Yanmei Shen, Like Yang, Tuo Zhang and Jia Ge *

Received 29th November 2020
Accepted 2nd January 2021

DOI: 10.1039/d0ay02186e

rsc.li/methods

Fluorescent carbon dots derived from natural biomass have received widespread attention in recent years due to their superior optical and chemical properties. In this work, we proposed a method to synthesize fluorescent nitrogen, sulfur, and phosphorus co-doped carbon dots (NSP-CDs) using biomass waste as a precursor. The blue emitting carbon dots were prepared from the seeds of green pepper, and Fe^{3+} ions could quench the fluorescence of NSP-CDs. Therefore, a fluorescent "turn-off" sensor based on NSP-CDs was constructed for the detection of Fe^{3+} ions. Further, NSP-CDs were evaluated as a fluorescent biosensor for the detection of Fe^{3+} in tap water and lake water samples, showing their potential value in practical applications. The cytotoxicity test further confirmed that NSP-CDs have good biocompatibility and can be extended to cell imaging and intracellular Fe^{3+} detection. The proposed method is simple, economical and green, which can meet the requirements of environmental monitoring and biological imaging.

1 Introduction

In 2004, Xu *et al.* reported carbon dots (CDs) for the first time.[1] Since then, CDs have received widespread attention from researchers in the fields of fluorescence sensing, biomedicine, energy, and nanocomposites.[2–6] As the primary element of carbon dots, carbon is an essential component of living organisms, which provides carbon dots with lower toxicity and good biocompatibility.[7] Studies have shown that the composition and surface functional groups of carbon dots are important factors affecting their luminescence and sensing properties.[8] Besides, heteroatom doping can improve the optical properties and quantum yield of CDs.[9–13] In general, doping with nitrogen atoms in CDs can improve the stability and fluorescence quantum yield of CDs.[14,15] Sulfur doping not only enhances the fluorescence intensity but also causes a redshift of the maximum absorption wavelength.[16] Then, nitrogen and sulfur are used as heteroatoms to prepare doped carbon dots.[17–19] However, many traditional methods for preparing co-doped CDs with these heteroatoms are expensive and not environmentally friendly. In terms of detection technology, fluorescence spectroscopy has greatly attracted people's interest due to its excellent high sensitivity, simplicity and rapid response, and it meets the needs of fast and sensitive detection.[20–22]

In recent years, the use of natural biomass as precursors to prepare fluorescent carbon dots has become a research hotspot. Hu *et al.* prepared S and N co-doped CDs by hydrothermal heating of water chestnut and onion.[23] Sahu *et al.* used orange juice as a precursor to prepare N-doped CDs.[24] Wang *et al.* prepared N-doped CDs from milk.[25] Chen *et al.* used garlic as a precursor to prepare N and S co-doped CDs.[26] And S and N co-doped carbon dots with tunable luminescence properties derived from hair fiber have also been demonstrated by Sun *et al.*[27] Natural materials are widely distributed in nature. Natural materials containing heteroatoms (N, S, P) are very suitable for preparing heteroatom-doped CDs. The use of natural resources to synthesize CDs has the advantages of low cost and environmental protection. Compared with physical and chemical methods, green synthetic methods have higher acceptability and will not cause chemical pollution.[28–30] From the perspective of the environment, material synthesis and sensing, it is very meaningful to synthesize carbon dots from biomass waste in a simple, economical and green way without the need for additional surface passivators. It not only avoids the use of expensive or toxic chemicals and complicated post-treatment processes, but also makes full use of resources, saving costs and achieving environmental protection. As the same time, most natural materials have intricate compositions, so carbon dots made of these materials usually have different surface groups and excellent properties, which is conducive to the better development and utilization of carbon dots.[31]

College of Chemistry, Green Catalysis Center, Henan Joint International Research Laboratory of Green Construction of Functional Molecules and Their Bioanalytical Applications, Zhengzhou University, Zhengzhou 450001, P. R. China. E-mail: jiage0630@hnu.edu.cn; Tel: +86-371-67783126

† Electronic supplementary information (ESI) available. See DOI: 10.1039/d0ay02186e

However, using food directly to synthesize carbon dots also has certain disadvantages. For example, in many parts of the world, food is in short supply, and it is a waste to use edible materials to synthesize carbon dots.

Green pepper is a common vegetable in all seasons, and it is also a food that we often eat in our daily life. Its consumption is enormous all over the world. Green peppers are rich in ascorbic acid, carbohydrates, carotenoids and other carbonaceous organic substances, so green peppers can be selected as a new carbon source to synthesize carbon dots. Moreover, green peppers are usually washed and the stems and seeds are removed when we eat them. The seeds and stems of the green peppers are generally treated as food waste, and turning them into valuable products can have significant economic and environmental benefits.

Herein, we report a simple, economical and green way to synthesize fluorescent N, S, P co-doped carbon dots (NSP-CDs) by a one-step hydrothermal method with the seeds of green pepper as precursors. The synthesis route is facile and eco-friendly, and the prepared NSP-CDs exhibit excellent optical properties, good biocompatibility and photo-stability. As shown in Scheme 1, NSP-CDs emit blue fluorescence with a quantum yield of 8.7%, and after adding Fe^{3+} ions, the fluorescence was quenched. This is because NSP-CDs are rich in phosphate groups, and Fe^{3+} ions can bind to the phosphate groups to form Fe–O–P bonds, resulting in the fluorescence signal of NSP-CDs being significantly quenched. This method was applied for the detection of Fe^{3+} ions in tap water and lake water. Besides, we also applied NSP-CDs for the detection of Fe^{3+} ions in living cells, indicating the potential application of NSP-CDs in bioimaging.

2 Experimental procedures

2.1 Preparation of the NSP-CDs

The NSP-CDs were synthesized through the hydrothermal method with green pepper seeds as precursors. Specifically, 4.0 g of green pepper seeds were added to 20 mL of ultrapure water, and then the mixture was transferred to an autoclave and heated it at 180 °C for 5 h. The NSP-CDs solutions were collected by centrifugation at 10 000 rpm for 20 min to remove large insoluble particles. The pale yellow transparent supernate solution was subjected to dialysis through a membrane (MWCO of 1 kD) for 24 h and the stable brown powder was collected by freeze-drying.

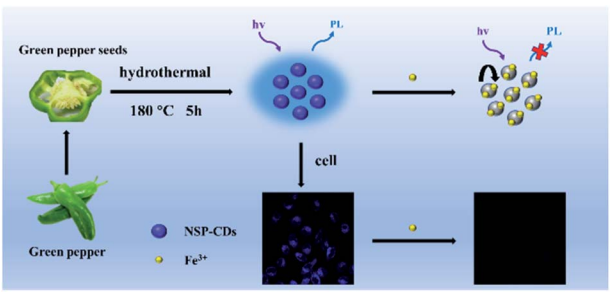

Scheme 1 Illustration of the formation process of NSP-CDs from green pepper seeds and their application in the detection of Fe^{3+}.

2.2 Detection of Fe^{3+} ions based on NSP-CDs

The detection of Fe^{3+} was carried out in ultrapure water. To put it simply, 200 μL NSP-CDs (500 μg mL^{-1}) were added to the centrifuge tube, and then different concentrations of Fe^{3+} ions were added and mixed thoroughly before testing. Subsequently, the fluorescence spectrum was recorded at an excitation wavelength of 330 nm.

The selectivity of Fe^{3+} sensing was confirmed by adding other common metal ion stock solutions (including Na^{+}, K^{+}, Ca^{2+}, Mg^{2+}, Zn^{2+}, Ni^{2+}, Co^{2+}, Mn^{2+}, Al^{3+}, Ag^{+} and Cu^{2+} ions), amino acids and small molecules (Pro, His, Lys, Thr, Arg, Gly, Hcy, Cys, Met, Leu, Ser, Val, BSA, glucose and sucrose) instead of Fe^{3+} in the same way. The concentrations of NSP-CDs and these species were 50 μg mL^{-1} and 1 mM, respectively.

2.3 Analysis of Fe^{3+} ions in environmental waters

Taking tap water and lake water as real samples, the practicality of the designed sensing method was investigated. The real water sample environment is more complicated and often contains a variety of large particles of impurities, so we filtered the water to remove impurities before testing. Subsequently, different concentrations of Fe^{3+} ions were added to the NSP-CDs solution containing 10% tap water or lake water, and the fluorescence emission spectrum was recorded.

3 Results and discussion

3.1 Characterization of the NSP-CDs

The structure and properties of NSP-CDs were studied by transmission electron microscopy (TEM), Fourier transform infrared spectroscopy (FT-IR), X-ray diffraction (XRD) and X-ray photoelectron spectroscopy (XPS). The morphology of NSP-CDs

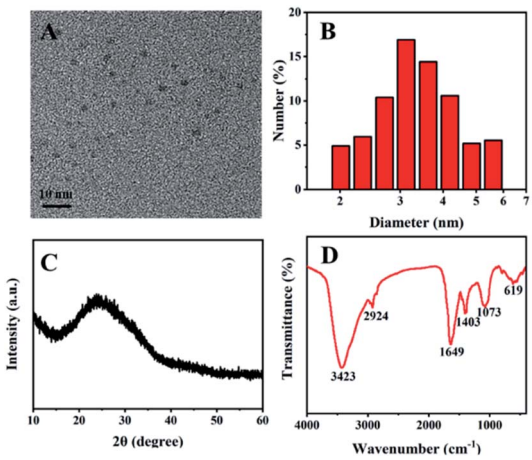

Fig. 1 (A) Typical TEM image and photograph of prepared NSP-CDs. (B) Particle size distribution of NSP-CDs. (C) X-Ray Diffraction (XRD) spectrum of NSP-CDs. (D) Fourier transform infrared (FT-IR) spectrum of NSP-CDs.

is approximately spherical and dispersion is relatively uniform in the TEM image (Fig. 1A). It can be seen from the particle size distribution diagram that the average particle size is about 3.2 nm (Fig. 1B). The XRD pattern shows that NSP-CDs have a distinct diffraction peak at 23.8°, indicating the amorphous structure of NSP-CDs (Fig. 1C). The FT-IR spectra of the NSP-CDs displayed the stretching vibrations for N–H/O–H (3423 cm^{-1}), C–H (2924 cm^{-1}), C=C/C=O (1649 cm^{-1}), C–N (1403 cm^{-1}), C–O–C/P–O (1073 cm^{-1}), and P=O/S=O (619 cm^{-1}) (Fig. 1D).[32–34] The above results indicate that the prepared CDs contain C, N, O, S and P elements.

The elemental compositions of NSP-CDs were studied by XPS characterization. The analysis results showed that five peaks appeared in the total spectrum, corresponding to the elements of carbon, nitrogen, oxygen, sulfur and phosphorus (Fig. 2A). The C 1s peak with a binding energy of 284.8 eV can be divided into four peaks, and the corresponding binding energies are 284.5 eV, 285.0 eV, 286.2 eV, and 288.0 eV, indicating that the surface of the NSP-CDs have C=C, C–S, C–N and C=O groups (Fig. 2B). Binding energies of N 1s peaks with a binding energy of 399.82 eV are 398.8 eV and 401.8 eV, corresponding to C–N–C and N–H groups (Fig. 2C). Two peaks of the O 1s spectrum are at 531.8 eV and 532.6 eV, which are attributed to the C=O and C–OH/C–O–C groups, respectively (Fig. 2D). The peaks of 167.9 eV and 169.0 eV in the S 2p graph correspond to S $2p_{3/2}$ and S $2p_{1/2}$, respectively (Fig. 2E).[35] The binding energies of 132.8 eV and 133.4 eV are attributed to P $2p_{3/2}$ and P $2p_{1/2}$, respectively (Fig. 2F).[36] The above characterization results show that we used the natural product green pepper seeds as precursor molecules for the successful preparation of NSP-CDs. Moreover, the material compositions of the as-prepared NSP-CDs were analyzed by energy-dispersive spectrometry (EDS), and elemental peaks representing C, N, O, S and P were observed (Fig. S1†).

3.2 Optical properties of the NSP-CDs

We investigated the photophysical properties of NSP-CDs through the UV-vis absorption spectrum and fluorescence spectrum. A broad absorption peak of the NSP-CDs aqueous solution appeared at 280 nm (Fig. 3A), which was assigned to the π–π* transition of aromatic sp^2 domains from the carbon core.[37] Moreover, the maximum excitation and emission peaks of NSP-CDs were located at 330 nm and 420 nm, respectively. And the inset showed that NSP-CDs emit bright blue fluorescence under UV light. We have also studied the fluorescence properties of NSP-CDs (Fig. 3B). When the excitation wavelength was increased from 310 nm to 380 nm (interval 10 nm), the fluorescence emission peak of NSP-CDs gradually red-shifted (from 400 nm to 460 nm). This showed that the emission wavelength of NSP-CDs had an obvious excitation-dependent behaviour.

In addition, the effects of ionic strength, pH and UV exposure time on the fluorescence intensity of NSP-CDs were studied. The fluorescence intensity of NSP-CDs remained basically unchanged in high-concentration NaCl solutions (Fig. S2†), which indicated that NSP-CDs are very stable under high-ion conditions. With the change of the pH environment (from pH 2.0 to pH 12.0), the fluorescence intensity of NSP-CDs was hardly affected, indicating that NSP-CDs have good pH

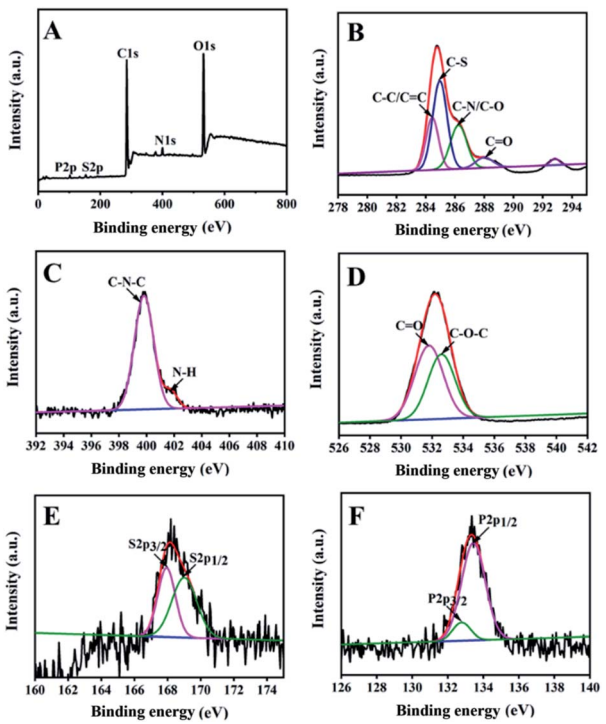

Fig. 2 (A) XPS spectra of NSP-CDs. (B–F) High-resolution XPS spectra of C 1s, N 1s, O 1s, S 2p and P 2p of NSP-CDs.

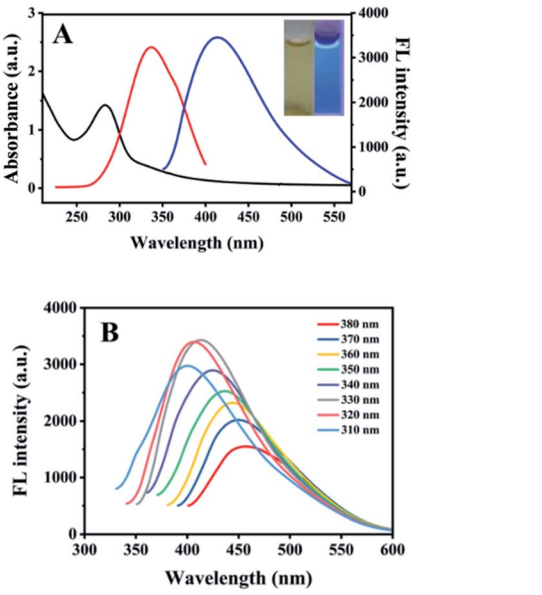

Fig. 3 (A) UV-vis absorption spectrum (inset on the left: photograph obtained under visible light) and optimal excitation and emission fluorescence spectra (inset on the right: photograph obtained under 365 nm UV light) of the NSP-CD aqueous solution; (B) fluorescence spectra of the NSP-CD aqueous solution under different excitation wavelengths.

stability (Fig. S3†). Under UV light for one hour, the fluorescence intensity remained basically unchanged, indicating that NSP-CDs have good photobleaching resistance (Fig. S4†). These results implied that NSP-CDs had excellent water-solubility and photo-stability, and could be used for biosensing and bioimaging.

3.3 Fluorescence detection of Fe^{3+} in solutions

First, we studied the feasibility of this sensing system. When Fe^{3+} was added to the NSP-CDs solution, the fluorescence of NSP-CDs was quenched (Fig. 4). Fe^{3+} could selectively bind to phosphonic acid-functionalized fluorene derivatives, due to the Fe^{3+} binding to them *via* the O-atoms of the phosphonic group.[38–40] In our work, the prepared NSP-CDs are rich in phosphate groups, and Fe^{3+} ions could bind to the phosphate groups to form Fe–O–P bonds, resulting in the fluorescence signal of NSP-CDs being significantly quenched. Then, we studied the effect of reaction time on the sensing system. After NSP-CDs reacted with Fe^{3+} ions for 30 seconds, the fluorescence intensity of NSP-CDs decreased by about 80%, indicating that the reaction process was relatively fast (Fig. S5†). Equilibrium was reached at 5 minutes, so 5 minutes was used for subsequent experiments. By collecting the changes in the fluorescence emission spectra of the experimental system, the response behaviour of NSP-CDs to different concentrations of Fe^{3+} ions was investigated. NSP-CDs emitted strong blue fluorescence, and when Fe^{3+} ions were added, the fluorescence intensity gradually decreased. When the concentration of Fe^{3+} ions was changed within the range of 0–1000 μM, the fluorescence intensity decreased, and the position of the fluorescence emission peak gradually redshifted, which may be due to the combination of NSP-CDs and Fe^{3+} ions to form a new complex (Fig. 5A). When the concentration of Fe^{3+} ions reached 1000 μM, the fluorescence quenching efficiency could reach more than 90%. As shown in Fig. 5B, the relative fluorescence intensity F_0/F and concentration of Fe^{3+} ions showed a good linear relationship in the concentration range of 1–500 μM (F_0 and F are fluorescence intensity values in the absence and presence of Fe^{3+} ions). The corresponding linear equation is $y = 0.0082\ x + 1.123$ ($R^2 = 0.9978$), and the detection limit calculated according to the 3σ rule is 0.1 μM. As shown in Table S1,† the detection limit of our proposed strategy is lower than that of other strategies, indicating the high sensitivity of NSP-CDs toward Fe^{3+} ion detection.

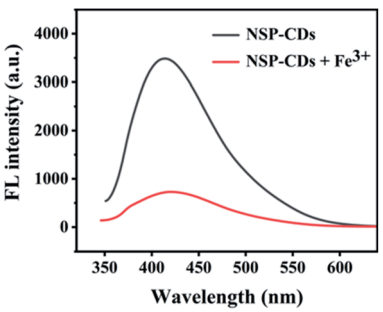

Fig. 4 Fluorescence spectra of NSP-CDs (black line) in the presence of 500 μM Fe^{3+} (red line).

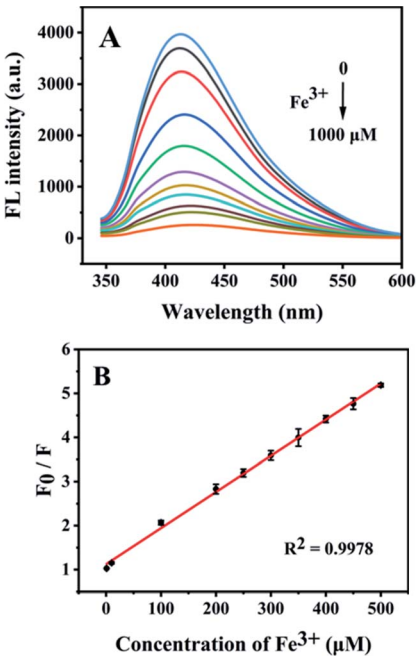

Fig. 5 (A) Fluorescence spectra of the NSP-CDs with increasing concentrations of Fe^{3+} (from top to bottom: 1, 10, 100, 200, 250, 300, 350, 400, 450 and 500 μM) under excitation at 330 nm. (B) Linear relationship of (F_0/F) *versus* the concentration of Fe^{3+} over the range of 1–500 μM.

We investigated the specificity of NSP-CDs in detecting Fe^{3+} ions. Fig. 6 shows the fluorescence intensity ratio F/F_0 of the NSP-CDs when incubated with various interfering ions (Na^+, K^+, Ca^{2+}, Mg^{2+}, Zn^{2+}, Ni^{2+}, Co^{2+}, Mn^{2+}, Al^{3+}, Ag^+ and Cu^{2+} ions). The results indicated that the NSP-CDs showed no obvious response. At the same concentration, Cu^{2+} ions can achieve a quenching effect of nearly 23%, and Fe^{3+} ions had the most prominent response effect with a quenching efficiency of about 80% (orange bars, Fig. 6A). Competition experiments were conducted by subsequently adding 500 μM Fe^{3+} to each solution (green bars, Fig. 6A). The above results indicated that interferents had no obvious influence on the fluorescence intensity ratio F/F_0 of the NSP-CDs. In addition, the response of NSP-CDs to various amino acids and small molecules (Pro, His, Lys, Thr, Arg, Gly, Hcy, Cys, Met, Leu, Ser, Val, BSA, glucose and sucrose) was also studied, and the results showed that the fluorescence signal of the system was basically unaffected (Fig. 6B). The above results showed that the NSP-CDs could be used as a selective Fe^{3+} fluorescent sensor. The high selectivity towards Fe^{3+} ions is due to the fact that Fe^{3+} more easily combines with the phosphate groups on the surface of the NSP-CDs to form Fe–O–P bonds than other metal ions.[38–40]

3.4 The sensing mechanism

The quenching process of fluorescence is usually divided into two methods: "dynamic quenching", when the excited state of the fluorescent molecule and the quenching agent molecule

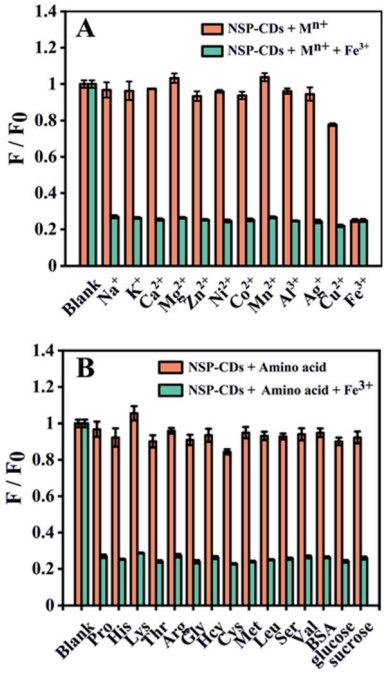

Fig. 6 (A) Fluorescence intensity response (F/F_0) of NSP-CDs toward various metal ions (Fe^{3+}, 500 μM; Na^+, K^+, Ca^{2+}, Mg^{2+}, Zn^{2+}, Ni^{2+}, Co^{2+}, Mn^{2+}, Al^{3+}, Ag^+, Cu^{2+}, 1 mM; orange bars) and the subsequent addition of 500 μM Fe^{3+} (green bars). (B) Fluorescence intensity response (F/F_0) of the NSP-CDs toward various amino acids and small molecules (Pro, His, Lys, Thr, Arg, Gly, Hcy, Cys, Met, Leu, Ser, Val, BSA, glucose and sucrose, 1 mM; orange bars) and the subsequent addition of 500 μM Fe^{3+} (green bars), where F_0 and F are the fluorescence intensities of the NSP-CDs in the absence and presence of Fe^{3+}, respectively.

collide, the fluorescent molecule returns from the excited state to the ground state by means of charge transfer or energy transfer, resulting in the disappearance of its fluorescence signal; "static quenching", combination of fluorescent molecules and quenching agent molecules to form a non-luminescent complex. At present, both quenching mechanisms can explain the cause of fluorescence quenching of fluorescent molecules. We researched the fluorescence lifetimes of NSP-CDs (black line) and a mixed system after adding Fe^{3+} to NSP-CDs (red line) (Fig. S6†). The fluorescence lifetimes of two curves are 3.80 ns and 3.72 ns respectively, indicated that the fluorescence quenching mechanism of NSP-CDs was static quenching.[41] In order to further confirm this inference, FT-IR and zeta-potential analysis were performed to prove that Fe^{3+} indeed complexed with the surface functional groups of NSP-CDs. Two curves, respectively, correspond to the infrared spectrum of NSP-CDs and addition of Fe^{3+} ions to NSP-CDs (Fig. S7†). Fe^{3+} ions combined with phosphate ions to break the P–O–P bond, and the absorption band at 1073 cm^{-1} corresponds to the vibration of the P–O bond. When Fe^{3+} ions were introduced into the system, the intensity of this band decreased. Meanwhile, after adding Fe^{3+}, the zeta potential value changed from −6.8 mV to +29.1 mV, which demonstrated that Fe^{3+} was selectively coordinated with the negative phosphorus group of the NSP-CDs (Fig. S8†).[42]

3.5 Detection of Fe^{3+} in real samples

Lake water and tap water were selected as real samples, and the sample solutions were filtered and then were diluted 10 times for subsequent experiments. As shown in Table 1, the standard recovery rates were 99.98–103.6%, and the relative standard deviations were between 1.99% and 5.19%. The results indicated that the proposed method shows good accuracy and reproducibility for Fe^{3+} ion detection in real samples.

3.6 Cytotoxicity test and cell imaging

In order to explore the biocompatibility of NSP-CDs, we studied the cytotoxicity of the NSP-CDs. As shown in Fig. S9,† after a higher concentration (200 μg mL^{-1}) of NSP-CDs solution was incubated with HeLa cells, HeLa cells could still maintain a survival rate of more than 90%, indicating that NSP-CDs have lower cytotoxicity. Hence the NSP-CDs can potentially be used for living cell imaging and other bio-medical applications.

As shown in Fig. 7, after NSP-CDs were incubated with HeLa cells at 37 °C for 4 h, blue emission appeared in the intracellular area. In addition, the bright field image of the cells after NSP-CDs treatment showed that the cell morphology was normal, indicating that NSP-CDs are biocompatible. To further study the

Table 1 Recovery tests for Fe^{3+} in tap water and lake water using the proposed assay ($n = 3$)

Samples	Added (μM)	Found (μM)	Recovery (%)	RSD (%)
Tap water	100	103.6	103.6	5.19
	150	150.4	100.3	1.99
	200	201.3	100.6	2.35
Lake water	100	99.98	99.98	3.99
	150	151.1	100.8	3.74
	200	200.6	100.3	2.57

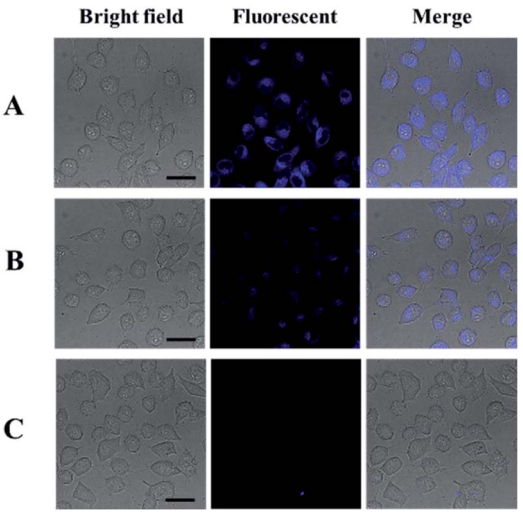

Fig. 7 Laser confocal imaging of HeLa cells under bright field, fluorescence and merged (A) with NSP-CDs; (B) NSP-CDs with 100 μM Fe^{3+} ions; (C) NSP-CDs with 200 μM Fe^{3+} ions. Scale bar is 20 μm.

application of NSP-CDs in monitoring intracellular Fe^{3+} ions, HeLa cells treated with NSP-CDs were incubated with 50 μM, 100 μM, and 200 μM Fe^{3+} for 30 minutes, respectively. With the addition of NSP-CDs, the cells showed bright blue fluorescence from the intracellular region, which clearly indicates the occurrence of cellular uptake of NSP-CDs (Fig. 7A). Then, the intracellular fluorescence of HeLa cells decreased after addition of 100 μM Fe^{3+} ions (Fig. 7B). Furthermore, the fluorescence properties of NSP-CDs were not observed after the addition of 200 μM Fe^{3+} ions (Fig. 7C), indicating that NSP-CDs could be used for cell imaging and detection of intracellular Fe^{3+} ions.

4 Conclusions

In summary, we proposed a strategy to prepare NSP-CDs using bio-waste green pepper seeds as precursors. The average size of the NSP-CDs was 3.2 nm, which showed good water solubility and strong excitation wavelength-dependent blue emission. At the same time, NSP-CDs have also been used for Fe^{3+} fluorescence sensing, and their quenching mechanism has been studied using fluorescence lifetime, infrared spectroscopy and zeta potential. In addition, NSP-CDs can easily enter the cytoplasm of cells for imaging and have good biocompatibility, indicating that they have broad application prospects as fluorescent biological probes. This strategy realizes the comprehensive utilization of biomass, has huge economic and environmental benefits and also expands the various applications of green and sustainable preparation of high-fluorescence nanomaterials.

Conflicts of interest

There are no conflicts to declare.

Acknowledgements

This work was supported by the National Natural Science Foundation of China (21505122) and Technology Plan Project (2019YFS0335), Sichuan Province, China.

Notes and references

1 X. Xu, R. Ray, Y. Gu, H. J. Ploehn, L. Gearheart, K. Raker and W. A. Scrivens, *J. Am. Chem. Soc.*, 2004, **126**, 12736–12737.
2 X. Geng, Y. Sun, Y. Guo, Y. Zhao, K. Zhang, L. Xiao, L. Qu and Z. Li, *Anal. Chem.*, 2020, **92**, 7940–7946.
3 S. Y. Lim, W. Shen and Z. Gao, *Chem. Soc. Rev.*, 2015, **44**, 362–381.
4 Y. Sun, H. Qin, X. Geng, R. Yang, L. Qu, A. N. Kani and Z. Li, *ACS Appl. Mater. Interfaces*, 2020, **12**, 31738–31744.
5 S. Zhu, X. Zhao, Y. Song, S. Lu and B. Yang, *Nano Today*, 2016, **11**, 128–132.
6 F. Yang, W. Bao, T. Liu, B. Zhang, S. Huang, W. Yang, Y. Li, N. Li, C. Wang, C. Pan and Y. Li, *Microchim. Acta*, 2020, **187**, 322.
7 S. Zhu, Q. Meng, L. Wang, J. Zhang, Y. Song, H. Jin, K. Zhang, H. Sun, H. Wang and B. Yang, *Angew. Chem., Int. Ed.*, 2013, **52**, 3953–3957.
8 N. Dhenadhayalan and K. C. Lin, *Sci. Rep.*, 2015, **5**, 10012.
9 P. Zhu, Z. Cheng, L. Du, Q. Chen and K. Tan, *Langmuir*, 2018, **34**, 9982–9989.
10 B. Han, T. Peng, M. Yu, C. Chi, Y. Li, X. Hu and G. He, *New J. Chem.*, 2018, **42**, 13651–13659.
11 Y. Wang, Q. Yue, L. Tao, C. Zhang and C. Z. Li, *Microchim. Acta*, 2018, **185**, 550.
12 X. Luo, W. Zhang, Y. Han, X. Chen, L. Zhu, W. Tang, J. Wang, T. Yue and Z. Li, *Food Chem.*, 2018, **258**, 214–221.
13 X. Zhu, J. Wang, Y. Zhu, H. Jiang, D. Tan, Z. Xu, T. Mei, J. Li, L. Xue and X. Wang, *Microchim. Acta*, 2018, **185**, 510.
14 H. Zhang, Y. Chen, M. Liang, L. Xu, S. Qi, H. Chen and X. Chen, *Anal. Chem.*, 2014, **86**, 9846–9852.
15 Z. X. Wang and S. N. Ding, *Anal. Chem.*, 2014, **86**, 7436–7445.
16 W. Kwon, J. Lim, J. Lee, T. Park and S. W. Rhee, *J. Mater. Chem. C*, 2013, **1**, 2002.
17 W. Wang, Y. C. Lu, H. Huang, A. J. Wang, J. R. Chen and J. J. Feng, *Sens. Actuators, B*, 2014, **202**, 741–747.
18 H. Ding, J. S. Wei and H. M. Xiong, *Nanoscale*, 2014, **6**, 13817–13823.
19 Y. Dong, H. Pang, H. B. Yang, C. Guo, J. Shao, Y. Chi, C. M. Li and T. Yu, *Angew. Chem.*, 2013, **125**, 7954–7958.
20 H. B. Wang, Y. Li, Y. Chen, Z. P. Zhang, T. Gan and Y. M. Liu, *Microchim. Acta*, 2018, **185**, 102.
21 H. B. Wang, Y. Li, H. Y. Bai and Y. M. Liu, *Sens. Actuators, B*, 2018, **259**, 204–210.
22 J. Ge, Y. Hu, R. Deng, Z. Li, K. Zhang, M. Shi, D. Yang, R. Cai and W. Tan, *Anal. Chem.*, 2020, **92**, 13588–13594.
23 Y. Hu, L. Zhang, X. Li, R. Liu, L. Lin and S. Zhao, *ACS Sustainable Chem. Eng.*, 2017, **5**, 4992–5000.
24 S. Sahu, B. Behera, T. K. Maiti and S. Mohapatra, *Chem. Commun.*, 2012, **48**, 8835.
25 L. Wang and H. S. Zhou, *Anal. Chem.*, 2014, **86**, 8902–8905.
26 Y. Chen, Y. Wu, B. Weng, B. Wang and C. Li, *Sens. Actuators, B*, 2016, **223**, 689–696.
27 D. Sun, R. Ban, P. H. Zhang, G. H. Wu, J. R. Zhang and J. J. Zhu, *Carbon*, 2013, **64**, 424–434.
28 G. Gedda, C. Y. Lee, Y. C. Lin and H. Wu, *Sens. Actuators, B*, 2016, **224**, 396–403.
29 W. Du, X. Xu, H. Hao, R. Liu, D. Zhang, F. Gao and Q. Lu, *Sci. China: Chem.*, 2015, **58**, 863–870.
30 L. Li, L. Li, C. P. Chen and F. Cui, *Inorg. Chem. Commun.*, 2017, **86**, 227–231.
31 R. Das, R. Bandyopadhyay and P. Pramanik, *Mater. Today Chem.*, 2018, **8**, 96–109.
32 C. Wang, D. Sun, K. Zhuo, H. Zhang and J. Wang, *RSC Adv.*, 2014, **4**, 54060–54065.
33 Y. Yang, D. Huo, H. Wu, X. Wang, J. Yang, M. Bian, Y. Ma and C. Hou, *Sens. Actuators, B*, 2018, **274**, 296–303.
34 D. Gu, L. Hong, L. Zhang, H. Liu and S. Shang, *J. Photochem. Photobiol., B*, 2018, **186**, 144–151.
35 Y. Zhao, S. Zou, D. Huo, C. Hou, M. Yang, J. Li and M. Bian, *Anal. Chim. Acta*, 2019, **1047**, 179–187.

36 H. Li, F. Q. Shao, S. Y. Zou, Q. J. Yang, H. Huang, J. J. Feng and A. J. Wang, *Microchim. Acta*, 2016, **183**, 821–826.
37 D. K. Dang, C. Sundaram, Y. L. T. Ngo, J. S. Chung, E. J. Kim and S. H. Hur, *Sens. Actuators, B*, 2018, **255**, 3284–3291.
38 C. Yi, W. Tian, B. Song, Y. Zheng, Z. Qi, Q. Qi and Y. Sun, *J. Lumin.*, 2013, **141**, 15–22.
39 C. Yi, B. Song, W. Tian, X. Cui, Q. Qi, W. Jiang, Z. Qi and Y. Sun, *Tetrahedron Lett.*, 2014, **55**, 5119–5123.
40 H. He, Q. Gan and C. Feng, *J. Appl. Polym. Sci.*, 2017, **134**, 45165.
41 Y. Liu, W. Duan, W. Song, J. Liu, C. Ren, J. Wu, D. Liu and H. Chen, *ACS Appl. Mater. Interfaces*, 2017, **9**, 12663–12672.
42 J. Shangguan, J. Huang, D. He, X. He, K. Wang, R. Ye, X. Yang, T. Qing and J. Tang, *Anal. Chem.*, 2017, **89**, 7477–7484.